Proceedings of ITC18,2008

Integrated Performance and Critical Issues Towards Steady-State Operation in JT-60U

YOSHITERU SAKAMOTO and the JT-60 team

Japan Atomic Energy Agency, 801-1, Mukouyama, Naka, Ibaraki-ken, 311-0193, Japan

This paper reports the integrated performance, achieved in JT-60U, towards the steady-state operation foreseen in ITER and DEMO reactor. Advanced tokamak plasmas with weak shear or reversed shear have been optimized to confront the critical issues such as the high-beta operation with high confinement, the compatibility of high-density operation with high confinement, and long sustainment with high non-inductive current drive. As a result, high-integrated performances were achieved in both plasma regimes. For example, high confinement reversed shear plasmas with high bootstrap current fraction exceeding no-wall beta limit are obtained in reactor relevant regime, where $\beta_N \sim 2.7$, $\beta_p \sim 2.3$ is achieved with reversed q profile with $q_{min} \sim 2.3$, and then $HH_{98y2} \sim 1.7$, $n_e/n_{GW} \sim 0.87$ and $f_{BS} \sim 0.9$ are also obtained at $q_{95} \sim 5.3$.

Keywords: advanced tokamak, integrated performance, DEMO reactor, high beta, high density, high confinement, long sustainment

1. Introduction

High fusion performances were achieved so far in JT-60U, which is one of the largest tokamak in the world. For example, the record values of fusion triple product $n\tau T = 1.53 \times 10^{21}$ m^{-3}skeV [1] and the DT equivalent fusion gain $Q_{DT}^{eq} = 1.25$ [2]. Towards steady-state operation of tokamak, however, high-integrated performance is required, where high values of confinement enhancement factor over ELMy H-mode scaling (HH_{98y2}), normalized beta (β_N), bootstrap current fraction of plasma current (f_{BS}), non-inductive driven current fraction of plasma current (f_{CD}), fuel purity, the ratio of radiation loss power to absorbed heating power (f_{rad}) and normalized electron density by Greenwald density limit (n_e/n_{GW}) should be sustained long time [3]. For example, ITER steady-state operation scenario foresees $HH_{98y2} = 1.61$, $\beta_N = 2.93$, $f_{BS} = 0.46$, $f_{CD} = 1.0$, fuel purity of 0.82, $f_{rad} = 0.53$ and $n_e/n_{GW} = 0.78$ [4]. Furthermore, other reactor relevant conditions are also important in which the operation region of $q_{95} \sim 5$, electron temperature nearly equal to ion temperature and low momentum input due to alpha heating.

In JT-60U, two types of advanced tokamak plasmas with an internal transport barrier (ITB) and an edge transport barrier (ETB) have been optimized towards high-integrated performance [5]. One is a high β_p H-mode plasma, the so-called a weak shear plasma, which is characterized by safety factor (q) profile with weak positive magnetic shear in the core region, the parabolic-type weak ITB and a higher beta limit compared with that of reversed shear plasmas. The other is a reversed shear H-mode plasma, which is characterized by q profile with negative magnetic shear in the core region, the box-type strong ITB and larger bootstrap current and higher confinement compared with those of weak shear plasmas.

Critical issues towards the high-integrated performance focused in this paper are as follows. First issue is simultaneous achievement of high beta and high confinement, because these performances directly enhance the fusion performance. Second issue is the compatibility of high density with high confinement. Since the large amount of particle fueling by gas puff degrades temperature in the core region, we should develop the high-density operation with keeping the high confinement. Third issue is long sustainment, where demonstration of steady-state plasma with high non-inductive current drive fraction over the characteristic timescales, for example energy confinement time (τ_E), current diffusion time (τ_R) and wall saturation time (τ_W) and so on, is required.

Progress of integrated performances achieved in weak shear and reversed shear plasmas on JT-60U is described in this paper and which is organized as follows. High-beta operation above no wall beta limit is described in section 2. High-density operation with high confinement is described in section 3. Long sustainment with high non-inductive current drive fraction is described in section 4. A summary is presented in section 5.

author's e-mail: sakamoto.yoshiteru@jaea.go.jp

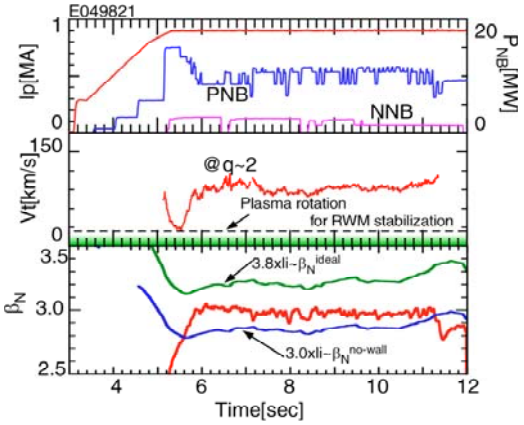

Fig.1 Waveforms of the stationary sustained weak shear plasma with wall stabilization.

2. High beta operation above no wall beta limit

The stability limit of ideal low n kink modes is significantly improved when a plasma is close to a perfectly conducting wall. However resistive wall modes (RWMs), which are a branch of ideal low n kink modes, are destabilized due to the finite resistivity of the conducting wall when the plasmas exceed no-wall beta limit due to the ideal low n kink modes. The RWM can be stabilized by using externally applied nonaxisymmetric magnetic field with coils [6] and/or by sufficient plasma rotation [7]. Recent experiments in JT-60U and DIII-D identified that a low toroidal rotation threshold for stabilizing RWM, where the toroidal rotation velocity at the low order rational surface plays important role [8, 9]. High beta experiments above no-wall beta limit were performed in weak shear and reversed shear plasma in JT-60U.

In weak shear plasma regime, high $\beta_N \sim 4$ was transiently achieved by wall stabilization [10]. Recently, quasi-steady state weak shear plasma with wall stabilization was obtained by utilizing the control of toroidal rotation velocity to keep above critical velocity [11]. Figure 1 shows the waveform of the stationary sustained weak shear plasma above no-wall beta limit, where $\beta_N \sim 3$ sustained for ~ 5s. In the discharge, low power of neutral beam (NB) heating was applied during Ip ramp-up phase to produce the weak positive shear configuration, and high power NB heating with negative ion-based neutral beam (N-NB) was injected to produce ITB. The β_N was sustained by using feedback control of stored energy via perpendicular NBs. The toroidal rotation velocity at q ~ 2 surface is much faster than the critical velocity ~ 20 km/s as shown in the figure. The no-wall beta limit is roughly indicated as 3.0 times the internal inductance, while the ideal wall beta limit as 3.8 times the internal inductance, which is confirmed by MARG2D code [12]. According to ACCOME code [13], which solves the inductive and non-inductive current density profiles that are consistent with plasma equilibrium, $f_{CD} > 0.8$ and $f_{BS} \sim 0.5$ were achieved. Since the large volume configuration was utilized for wall stabilization, lower confinement ($HH_{98y2} \sim 0.8$) is attributed to the lack of strong central heating. The duration is determined by the increase of no-wall beta limit due to gradual penetration of inductive field. Furthermore, some MHD instabilities cause the disruption in the high beta weak shear plasmas above no-wall beta limit. In particular, n = 1 bursting mode and slowly growing mode as a RWM precursor have been observed [11]. The bursting mode, so-called energetic particle driven wall mode (EWM) [*], is the energetic particle branch as the results of the interaction between the energetic particle and a marginally stable RWM, and then directly triggers RWM despite of enough toroidal rotation velocity for RWM stabilization. The slowly growing mode, which has longer growth time than the resistive wall time, makes toroidal rotation velocity and its shear at the rational surface reduce, and then the RWM is destabilized.

In reversed shear plasma regime, typical waveforms of the discharge with above no-wall beta limit are shown in Fig. 2, where the plasma parameters are as follows: plasma current $I_p = 0.8$MA, toroidal magnetic field $B_T = 2.0$T, $q_{95} \sim 5.3$ and the ratio of the wall radius to the plasma minor radius d/a ~ 1.3 [15]. The value of q_{95} is actually close to the design parameter of DEMO reactors. The discharge was established under the low momentum input condition expected in DEMO reactors, where tangential neutral beams (NBs) were injected by balanced

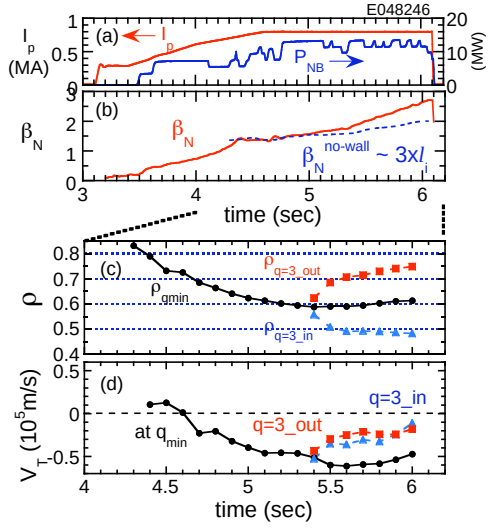

Fig.2 Waveforms of the wall-stabilized reversed shear discharge.

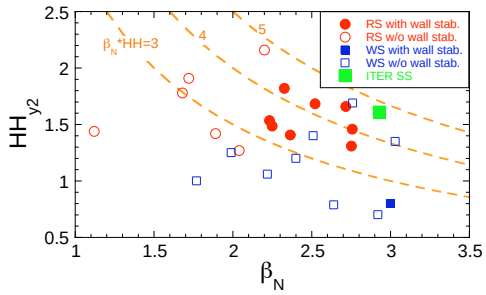

Fig.3 Simultaneous achievement of high normalized beta and high confinement.

way in which the injected power of co-tangential NBs is similar to that of ctr-tangential NBs. The normalized beta increased continuously by following the stored energy feedback control. However, the discharge was terminated by disruption at t ~ 6.1s. The MHD instability (n = 1) was observed just before the disruption, of which growth time is the order of the resistive wall time (τ_W ~ 10ms), suggesting RWM. In this discharge, β_N ~ 2.7 was achieved just before disruption, and the achieved high β_p ~ 2.3 leads to high f_{BS}. The achieved value of β_N is much higher than reversed shear plasmas with β_N ~ 1.7 - 2.2 at d/a ~ 1.5. The no-wall beta limit is estimated at about three times the internal inductance as shown in the figure. Actually, the detail analysis of MHD stability using the MARG2D code indicates that the ideal wall beta limit is β_N ~ 2.9 and the no-wall beta limit is ~1.9, resulting C_β ~ 0.8, where $C_\beta = (\beta_N - \beta_N^{\text{no-wall}}) / (\beta_N^{\text{ideal-wall}} - \beta_N^{\text{no-wall}})$. It should be noted that values of q such as q_{95} and q_{min} is very similar to those of ITER steady-state scenario (VI) for strong negative shear in which q_{95} ~ 5.4, q_{min} ~ 2.3 and q(0) ~ 5.9 are expected [4]. Thanks to ITBs, high confinement enhancement factor HH_{98y2} ~ 1.7 was obtained at high normalized density (n_e/n_{GW} ~ 0.87), and the ratio of electron and ion temperatures was T_e/T_i ~ 0.9 at the center. Furthermore, extremely high bootstrap current fraction of ~ 92% is obtained in the plasma, which is evaluated from ACCOME code. The RWM became unstable when toroidal rotation velocities at q = 3 surface decreased to the critical toroidal rotation velocity as shown in Fig. 2(d). By comparison of balanced- and co-injected discharges, the toroidal rotation velocity at outer q = 3 surface might play the important role for RWM stabilization.

Figure 3 shows simultaneous achievement of high beta and high confinement in both weak shear and reversed shear plasmas with/without wall stabilization. Beta limit was improved by RWM stabilization, especially in reversed shear plasmas with keeping high confinement. The high value of β_N ~ 3 was achieved with high HH_{98y2} ~1.5 in both plasma regimes, which is expected in ITER steady-state operation scenario. In weak shear plasmas, high β_N and high confinement was obtained even without wall stabilization as shown in the figure. Since the large volume configuration was utilized for wall stabilization discharges, lower confinement in the weak shear plasma with wall stabilization is attributed to the lack of strong central heating.

3. High-density operation with high confinement

Although the high-density operation above Greenwald density is preferable in DEMO reactors, confinement degradation was observed in the ELMy H-mode plasmas without ITBs [16]. In the plasmas with ITB, strong central heating is required for sustaining high confinement especially in weak shear plasmas. However it is difficult to keep a centrally peaked heating profile at high density due to the attenuation of neutral beam for heating.

Figure 4 shows the comparison of high-density operation in weak shear plasma discharge with pellet injection and with gas fueling [17], where the electron density was enhanced up to n_e/n_{GW} ~ 0.7 under the conditions of B_T = 3.6 T, I_p = 1.0 MA, q_{95} ~ 6.5, δ ~ 0.45 and q_{95} ~ 6.5. The pellets were injected from high field side. In addition, negative-ion based neutral beam (N-NB), which have high beam energy (~360 keV), was injected at high-density phase in order to keep a centrally peaked heating profile. In the pellet-injected discharge, the confinement enhancement factor over the L-mode scaling (H_{89PL}) stays almost constant even with increasing electron density, as shown in Fig. 4**(a)**, where HH_{98y2}

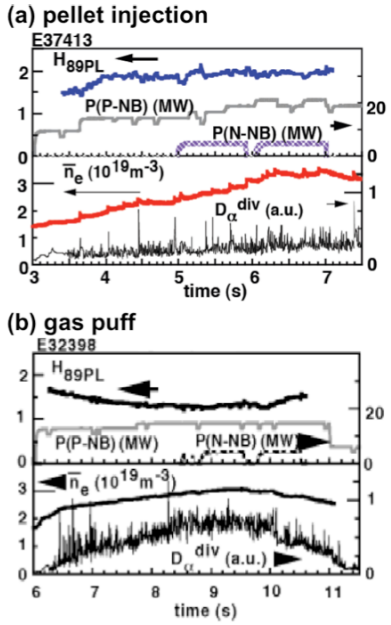

Fig.4 Waveforms of high-density operation by utilizing (a) pellet injection and (b) gas puff.

=1.05, β_N =2.2 and f_{BS} ~ 60% was simultaneously achieved at n_e/n_{GW} ~0.7. On the other hand, H_{89PL} decreases with increasing electron density in the gas fueled discharge as shown in Fig. 4(b). The ITBs in temperature profile were sustained and the density profile was peaked in the pellet-injected discharge, while the ITBs produced in the early phase disappeared in the gas-fueled discharge. One of the differences is seen in the pedestal parameter. The electron density at the pedestal is almost similar in both discharges, while the temperatures at the pedestal in the pellet-injected discharge are higher than that in the gas-fueled discharge. The pedestal temperature and density increases gradually in time in the pellet-injected discharge, where the core-edge parameter linkage plays an important role [17]. On the other hand, the temperature decreases with increasing density, which leads to decrease in the core temperatures and the energy confinement.

In reversed shear plasma regime, on the other hand, stronger ITBs are produced including electron density profile. The wide ITB radius can contribute the high-density operation with keeping high confinement characteristics. Figure 5 shows the electron density profile normalized to the Greenwald density in the high-density reversed shear plasma at before ITB formation and at fully developed ITB phase [18]. Here, B_T = 2.5T, I_p ~ 1.0MA, q_{95} ~ 6.1, and NB and LHRF heating were utilized. It should be noted that the density increases with NB fueling only. The density profile changes from relatively flat to a broad central peaked profile, where the density inside ITB increases, while the edge density remains almost constant. Although the edge electron density is smaller than $0.4n_{GW}$, the central electron density largely exceeds n_{GW} due to the wide radius of ITB. Therefore the high n_e/n_{GW} is obtained due to the peaked density profile inside the wide ITB. Thanks to ITBs, HH_{98y2} =1.3, β_N ~ 2 and f_{BS} ~ 70% were simultaneously achieved at n_e/n_{GW} = 1.1. It should be

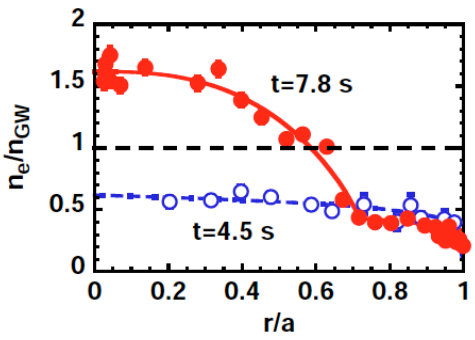

Fig.5 Profiles of electron density normalized by Greenwald density obtained in high-density reversed shear plasma.

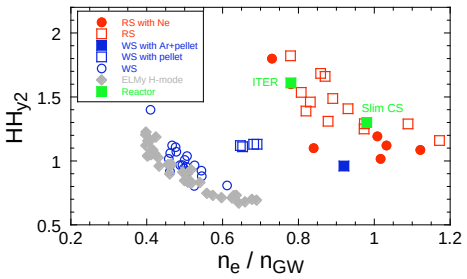

Fig.6 Compatibility of high density and high confinement in weak shear and reversed shear plasmas together with ELMy H-mode.

mentioned that the pedestal pressure is lower than that in the ELMy H-mode plasmas, and the core-edge parameter linkage is weak compared to weak shear plasmas.

Figure 6 shows the compatibility of high density and high confinement in both weak shear and reversed shear plasmas, where standard ELMy H-mode and impurity seeded plasmas [18] are also shown. Basically confinement performance is degraded with increasing n_e/n_{GW} in ELMy H-mode, weak shear and reversed shear plasmas. High-density operation region is expanded in weak shear plasmas with small degradation of confinement property by utilizing capability of density profile control such as pellet injection as described above, and impurity seeding with Argon, and then the high confinement region of HH_{98y2} > ~ 1 was achieved up to n_e/n_{GW} ~ 0.9. Furthermore, high-density operation region at n_e/n_{GW} ~ 1, foreseen in ITER steady-state operation scenario and DEMO reactor such as Slim CS, was obtained in reversed shear plasmas with very high confinement property (HH_{98y2} = 1.3 -1.7). In addition to high-density operation, high radiation loss fraction (f_{rad} > 0.9) was also obtained in the cases of impurity-seeded discharge. It is noted that HH_{98y2} ~ 0.95 at n_e/n_{GW} ~ 0.7 was obtained so far under the wall saturated condition, which is expected in steady-state plasmas [19].

4. Long sustainment with high non-inductive current drive fraction

Towards steady state operation of tokamak, the long sustainment of plasmas with full non-inductive current drive condition should be demonstrated. Critical issues for long sustainment are avoidance of neoclassical tearing modes in weak shear plasmas and the disruption in reversed shear plasmas.

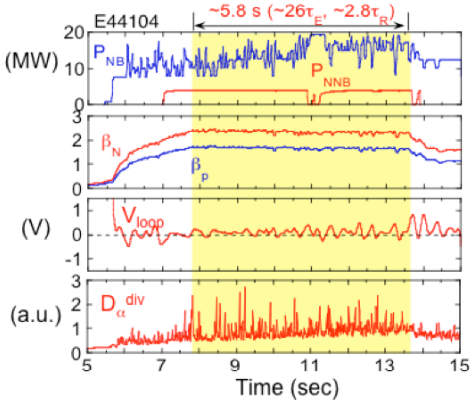

Fig.7 Waveforms of long sustained weak shear plasma with nearly full CD.

In the weak shear plasma regime, suppression of NTMs was demonstrated by electron cyclotron current drive [20]. However it is required for the complete avoidance of the NTM with m/n = 3/2 that the value of q in the whole plasma region is beyond 1.5. Typical waveform of such a scenario is shown in Fig. 7 [21], where I_p = 1 MA, B_T = 2.4 T, κ = 1.44, δ = 0.5 and q_{95} ~ 4.5. The plasma with β_N ~ 2.4 (β_p ~ 1.7) has been sustained for 5.8 s. This duration corresponds to ~ 26 τ_E and ~2.8 τ_R. Loop voltage was reduced near zero, which indicates the nearly full non-inductive current drive condition. The analysis of non-inductive current drive indicates that f_{BS} ~ 50-43% and f_{BD} ~ 52-47% were obtained. The sustained duration was determined by the pulse length of N-NB (~ 4 MW, ~ 6.5 s). In this discharge, HH_{98y2} ~1.0 was obtained at n_e/n_{GW} ~ 0.54. It should be emphasized that no NTM was observed in this discharge by the optimization of q profile.

In reversed shear plasma regime, one of the difficulties to obtain a long sustainment is avoidance of disruption due to the lower beta limit without wall stabilization. The reversed shear q profile gradually changes towards the stationary condition, where the value of q in core plasma region, including q_{min} and its location, decreases continuously due to the penetration of inductive current. Therefore the value of q_{min} passes through integer values until reaching stationary condition. Then the discharges frequently terminate by disruption when q_{min} goes across the integer values. In order to avoid disruptions, the pressure gradient at the ITB should be decreased when the plasma becomes unstable. The technique of the control of the ITB strength had been developed in JT-60U reversed shear discharges by the control of toroidal rotation, where local reduction of E_r shear affects the whole ITB layer [22]. For the long sustainment of the reversed shear plasmas with large f_{BS} under nearly full non-inductive current drive condition, we attempted the toroidal rotation control to avoid a

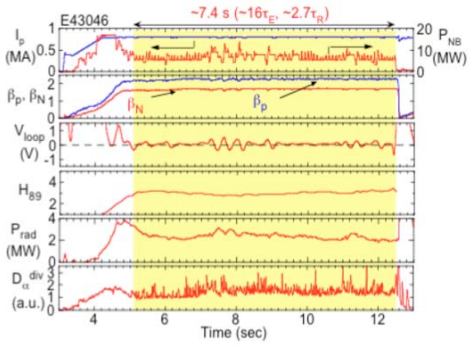

Fig.8 Waveforms of long sustained reversed shear plasma with nearly full CD.

disruption. Typical waveform of the long sustained reversed shear discharge are shown in Fig. 8, where I_p = 0.8 MA, B_T = 3.4 T, q_{95} ~ 8.3, κ_x = 1.6, δ_x = 0.42 [21]. Utilizing the feedback control of the stored energy by the perpendicular NBs, β_N ~ 1.7 (β_p ~ 2.4) was maintained from t ~ 5.1 s until the end of the NB heating (t = 12.5 s). Loop voltage decreased to nearly zero and was kept nearly constant, which indicates the nearly full non-inductive current drive condition. The high HH_{98y2} of ~1.9 was also maintained thanks to ITBs at n_e/n_{GW} ~ 0.6. According to ACCOME code, f_{CD} > 0.9 and f_{BS} ~ 0.75 were achieved. In this discharge, toroidal rotation control for pressure gradient control was applied during t = 7 – 8s at q_{min} being 4, where ctr-NB was switched off, and then the disruption was successfully avoided. The sustained duration of f_{BS} ~ 0.75 is ~ 7.4 s, which corresponds to ~ 16 τ_E and ~ 2.7 τ_R. At the stationary phase, the profile of measured total current density agrees closely with that of non-inductive current density, which implies the plasma approached the stationary condition.

Figure 9 shows progress of long sustainment of weak shear and reversed shear plasmas with high f_{BS}. By optimizing profiles of current and pressure, the sustained duration of both plasma regimes is extended under the nearly full non-inductive current drive condition. The plasmas with high f_{BS} expected in ITER steady state scenario and DEMO reactor is sustained for longer than current diffusion time scale, which is typically ~ 2 s in JT-60U. Durations are limited by pulse length of NB or N-NB.

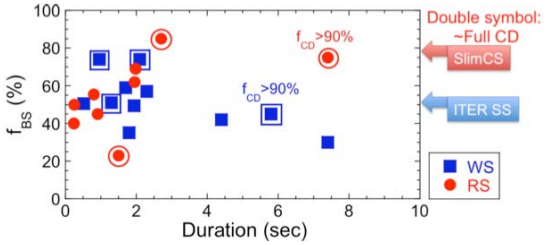

Fig.9 Progress of long sustainment of high bootstrap current fraction plasmas.

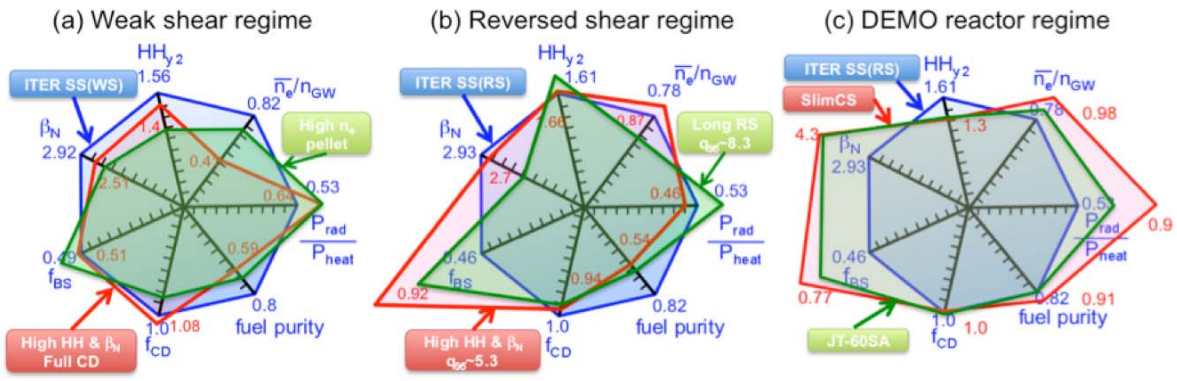

Fig. 10 Integrated performance achieved in (a) weak shear plasmas and (b) reversed shear plasmas. (c) Comparison of integrated performance among ITER, Slim CS and JT-60SA.

5. Summary

JT-60U tokamak optimized weak shear and reversed shear plasmas towards steady-state operation of tokamak and demonstrated (1) high beta and high confinement simultaneously, (2) compatibility of high density with high confinement, and (3) long sustainment under the nearly full non-inductive current drive condition. As the results, high-integrated performances were achieved in both plasma regimes. Achieved integrated performance in weak shear and reversed shear plasmas is shown in Fig. 10(a) and 10(b) together with the design parameter of the ITER steady-state scenarios [4]. In weak shear plasma regime, the discharge with high confinement and high beta plasma under the full non-inductive current drive condition [3] and the discharge with high density produced by pellet injection are shown in the figure. In reversed shear plasma regime, the discharge with high confinement and high beta plasma at reactor relevant q_{95} ~ 5.3 and the long pulse discharge at high q_{95} ~ 8.3 are shown in the figure. In both plasma regimes, high-integrated performance compared to ITER steady-state scenario was achieved. However some parameters are not satisfied simultaneously. And also long sustainment is still one of the remaining issues.

Concerning DEMO reactor, Slim CS [23] is one of the examples of economical and compact DEMO reactor with high β_N ~ 4.3 and high f_{BS} ~ 0.77. Figure 10(c) shows comparison of integrated performance among ITER steady state scenario, Slim CS and JT-60SA [24]. There are large gaps in design parameter between Slim CS and ITER, especially in β_N, f_{BS} and f_{rad}. JT-60SA will address the key issues for DEMO, as satellite tokamak of ITER, where demonstration of high beta operation by RWM control coils, and heat and particle control with divertor pumping capability. Then we hope ITER scenario can be improved by results of JT-60SA.

Acknowledgments

The authors would like to acknowledge the members of the Japan Atomic Energy Agency who have contributed to the JT-60U projects.

References

[1] S. Ishida et al., Proc. 16th Int. Conf. Plasma Physics and Controlled Nuclear Fusion Research, Montreal, Canada, October 7-11, 1996, Vol. 1, p. 315, International Atomic Energy Agency (1997).
[2] T. Fujita et al., Nucl. Fusion **39**, 1627 (1999).
[3] Y. Kamada and the JT-60 team, Nucl. Fusion **41**, 1311 (2001).
[4] Plasma Performance Assessment 2004 section 3.4, ITER Technical Basis ITER EDA Documentation Series.
[5] Y. Kamada et al., Fusion Science and Technology **42**, 185 (2002).
[6] C. M. Bishop, Plasma Phys. Control. Fusion **31,** 1179 (1989).
[7] A. Bondeson and Ward, D.J. Phys. Rev. Lett. **72**, 2709 (1994).
[8] M. Takechi et al., Phys. Rev. Lett. **98**, 055002 (2007).
[9] H. Reimerdes et al., Phys. Rev. Lett. **98**, 055001 (2007).
[10] M. Takechi et al., Proc. 21st Int. Conf. on Fusion Energy (Chengdu, 2006) (Vienna: IAEA) EX/7-1Rb.
[11] G. Matsunaga et al., Proc. 22nd Int. Conf. on Fusion Energy (Geneva, 2008) (Vienna: IAEA) EX/5-2.
[12] Tokuda, S. and Watanabe, T., Phys. Plasmas **6**, 3012 (1999).
[13] Tani, K., et al., J. Comput. Phys. **98**, 332 (1992).
[14] G. Matsunaga et al., submitted to Phys. Rev. Lett.
[15] Y. Sakamoto et al., Proc. 22nd Int. Conf. on Fusion Energy (Geneva, 2008) (Vienna: IAEA) EX/1-1.
[16] H. Urano et al., Plasma Phys. Control. Fusion **44**, 11 (2002).
[17] Y. Kamada et al., Plasma Phys. Control. Fusion **44**, A279 (2002).
[18] H. Takenaga et al., Nucl. Fusion **45**, 1618 (2005).
[19] N. Asakura et al., Proc. 22nd Int. Conf. on Fusion Energy (Geneva, 2008) (Vienna: IAEA) EX/4-4Ra.
[20] A. Isayama et al., Nucl. Fusion **43** 1272 (2003).
[21] Y. Sakamoto et al., Nucl. Fusion **45**, 574 (2005).
[22] Y. Sakamoto et al., Nucl. Fusion **41** 865 (2001).
[23] K. Tobita et al., Nucl. Fusion **47**, 892 (2007).
[24] T. Fujita et al., Nucl. Fusion **47**, 1512 (2007).